

# How hydrogen bonding affects ligand binding and fluxionality in transition metal complexes: a DFT study on interligand hydrogen bonds involving HF and H<sub>2</sub>O

Eric Clot,<sup>\*a</sup> Odile Eisenstein<sup>a</sup> and Robert H. Crabtree<sup>b</sup>

<sup>a</sup> LSDSMS (UMR 5636), Case Courrier 14, Université de Montpellier 2, 34095 Montpellier cedex 5, France. E-mail: clot@lsd.univ-montp2.fr

<sup>b</sup> Department of Chemistry, Yale University, New Haven, CT 06520-8107, USA. E-mail: robert.crabtree@yale.edu

Received (in Strasbourg, France) 16th August 2000, Accepted 10th October 2000

First published as an Advance Article on the web 1st December 2000

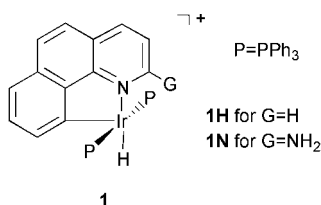
DFT calculations (B3PW91) predicted structures for hydrogen-bonded complexes of type Ir(H)(L)(bq-G)(PH<sub>3</sub>)<sub>2</sub><sup>q+</sup> (bq-H = benzo[h]quinoline-10-yl, L = empty site, FH or OH<sub>2</sub>; G = H or NH<sub>2</sub>, q = 1; L = F<sup>-</sup>, G = NH<sub>2</sub>, q = 0), which are either too unstable for X-ray crystallography study, or for which the crystal structure does not allow H atom positions reliably to be located. The work shows how the two-point binding site provided by the bq-NH<sub>2</sub> complex is ideal for HF but not for H<sub>2</sub>O binding, thus stabilizing the former to the extent that it can be observed by NMR at low temperature. Fluxionality in the aqua complex is fully interpreted by location of the appropriate TS. One such TS is strongly stabilized by hydrogen bonding leading to rapid exchange of NH<sub>2</sub> positions even at -80 °C. An improved ligand is suggested for stabilizing an HF complex.

## Introduction

Interaction energies in chemistry go from the weak van der Waals bond (100 cm<sup>-1</sup> for D<sub>0</sub> in Ar·H<sub>2</sub>O)<sup>1</sup> to the strong covalent bond (150 kcal mol<sup>-1</sup> for C-F bond in C<sub>6</sub>F<sub>6</sub>).<sup>2</sup> The directionality and intermediate interaction energy of the hydrogen bond allow creation of specific interactions in crystal engineering and supramolecular architecture;<sup>3-5</sup> theoretical studies on weak hydrogen bonds have been reviewed recently.<sup>6</sup>

Multifunctional ligands with reactive groups not involved in metal-ligand binding are of particular interest when they contain lone pairs unable to bind directly to the metal, but able to hydrogen bond to an adjacent ligand.<sup>7,8</sup> If properly placed, these groups could have effects similar to those of hydrogen-bonding residues in the active site cavity of metalloenzymes which are believed to contribute to the acceleration of enzyme reactions by transition-state stabilization.<sup>9</sup>

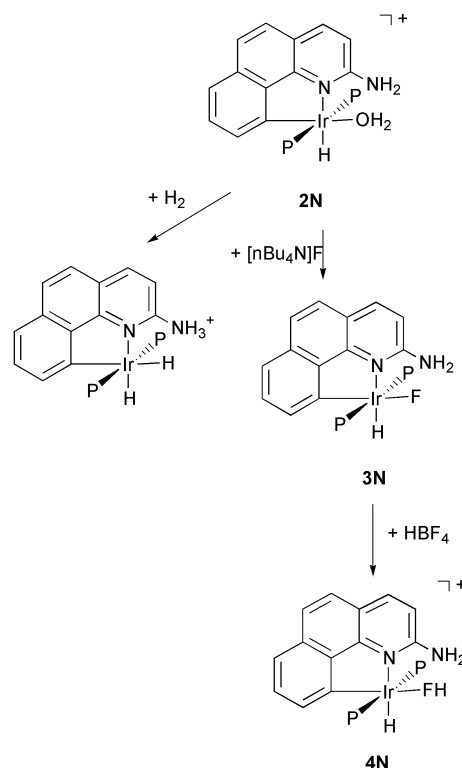
A simple example is shown as **1** below, where G can be either H (denoted **1H**) or a pendant amino group NH<sub>2</sub> (denoted **1N**) capable of hydrogen bonding to an incoming ligand L' bearing acidic protons (HF, H<sub>2</sub>O, for example). In prior work we have shown how water binds to **1H** to yield the aqua complex Ir(H)(H<sub>2</sub>O)(bq-H)(PPh<sub>3</sub>)<sub>2</sub><sup>+</sup> **2H** (bq-H = benzo[h]quinolin-10-yl) that can reversibly bind H<sub>2</sub> with loss of H<sub>2</sub>O.<sup>10,11</sup>

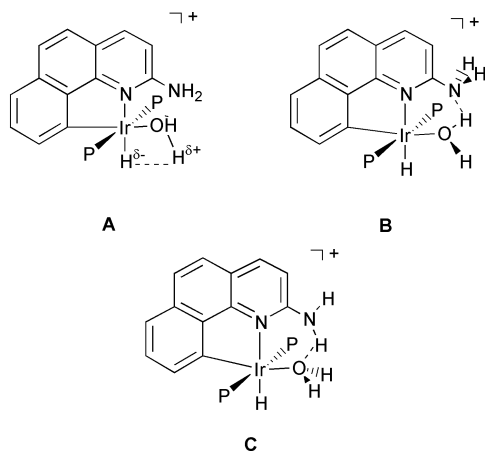


In the case of G = NH<sub>2</sub>, the aqua complex Ir(H)(H<sub>2</sub>O)(bq-NH<sub>2</sub>)(PPh<sub>3</sub>)<sub>2</sub><sup>+</sup> **2N** reacts with H<sub>2</sub> to give reversible heterolytic cleavage of H<sub>2</sub> not seen for **2H** (Scheme

1).<sup>12</sup> Moreover, the complex **2N** reacts rapidly with [nBu<sub>4</sub>N]F to give the fluoride complex **3N** (Scheme 1).<sup>13,14</sup>

Ligand substitution in metal fluoro complexes is subject to acid catalysis and the intermediacy of transient HF complexes was proposed<sup>15</sup> but experimental support was never obtained in prior studies. Fully characterized halogenocarbon complexes of type L<sub>m</sub>M-X-R (X = halide, R = alkyl or aryl) have been known for some time,<sup>16</sup> but the corresponding hydrogen





Scheme 2

halide complexes ( $R = H$ ,  $X = F$ ) have only been reported very recently.<sup>13,14,17</sup> Two bifluoride complexes,  $\text{Mo}(\text{PMe}_3)_4(\text{H}_2\text{F})(\text{FHF})$ <sup>18</sup> and *trans*- $\text{Ru}(\text{dmpe})_2(\text{H})(\text{FHF})$ ,<sup>19</sup> have also been characterized very recently by X-ray crystallography. In both cases the bifluoride ligand is  $\eta^1$ -bonded to the metal with an  $\text{M}-\text{F}\cdots\text{F}$  angle of 134 and 130°, respectively.<sup>20</sup> The hydrogen-bond within the coordinate bifluoride is asymmetric and less strong than in free  $\text{FHF}^-$ .

The HF complex **4N** is obtained by protonation of **3N** ( $\text{HBF}_4 \cdot \text{Et}_2\text{O}$ ) and has so far only been detected spectroscopically and at low temperature (Scheme 1). The critical observation was the finding of a  $J_{\text{HF}}$  value of 440 Hz, characteristic of hydrogen bonded HF. The pendant group  $\text{NH}_2$  is believed to interact with the HF ligand through hydrogen bonding to give overall two point binding via an  $\text{Ir}-\text{F}$  coordinate bond and an  $\text{N}\cdots\text{HF}$  hydrogen bond. With the stabilization of an HF complex, we now have experimental support for the presence of such intermediates in acid catalysed substitution and also a new ligand type.

Since the HF complex decomposes with loss of HF above  $-30^\circ\text{C}$ , no crystal structure is available and so the metric parameters of this new ligand type were still unknown. Efforts to make stabler derivatives having failed, we turn here to DFT (B3PW91) studies to predict the static structure expected for the new ligand. Being difficult to locate with X-ray diffraction the presence of H is often inferred from IR and NMR spectroscopic observations. Theory is one of the most powerful tools available to characterize the geometry of hydrogen bonded species and an accurate determination of the hydrogen atom positions is provided by DFT calculations.<sup>21</sup> The aqua complex **2N** provides a stringent test of the DFT methodology with three types of hydrogen bonding situations in competition (Scheme 2).

The aim of this paper is thus to explore computationally the structure and reactivity of the complexes between **1** and ligands like  $\text{H}_2\text{O}$ ,  $\text{F}^-$  or HF. Emphasis will be put on the role of G and thus on how hydrogen bonding helps in stabilizing particular geometries and in determining reactivity. One of our goals is to use DFT calculations to analyse the trends in binding energies between the metal fragment **1** and ligands like  $\text{H}_2\text{O}$  or HF as a function of pendant group G.

## Computational details

All calculations have been performed within the framework of Density Functional Theory (DFT) with the GAUSSIAN 98 set of programs.<sup>22</sup> The B3 hybrid exchange potential of Becke<sup>23</sup> was used in conjunction with the PW91 correlation potential of Perdew and Wang.<sup>24</sup> The relativistic Effective Core Potential (RECP) of the Stuttgart group was used for Ir with the associated (8s7p5d)/[6s5p3d] basis set augmented with an f function ( $\alpha = 1.0$ ).<sup>25</sup> The phosphorus atoms were also treated with Stuttgart's RECPs and the associated basis

set,<sup>26</sup> augmented by a d function ( $\alpha = 0.387$ ). A 6-31G(d,p) basis set was used for the hydride, the fluoride, both atoms (C and N) linked to Ir, and for the atoms of the G group ( $G = \text{H}$  or  $\text{NH}_2$ ). For the remaining atoms a 6-31G basis set was used.

Geometry optimizations without any symmetry constraints were performed on model systems where the three conjugated rings of the bq-G ( $G = \text{H}$  or  $\text{NH}_2$ ) ligand were explicitly considered. The only difference between the experimental and the calculated molecules lies in the use of  $\text{PH}_3$  to represent the phosphine ligands. This turns out to be a reasonable simplification since the electronic influence of  $\text{PPh}_3$  is rather well reproduced by  $\text{PH}_3$  according to the respective Tolman electronic factors ( $2069\text{ cm}^{-1}$  for  $\text{PPh}_3$  vs. estimated  $2081\text{ cm}^{-1}$  for  $\text{PH}_3$ ).<sup>27</sup> We will therefore not introduce an additional labeling scheme to distinguish between experimental and theoretical systems. This study being mostly theoretical, we will explicitly indicate when we refer to experimental results.

The nature of all located extrema was checked through analytical computations of the vibrational frequencies. The binding energy  $\Delta_{\text{bind}}^{\text{X}} E(L')$  of the ligand  $L'$  in the complex **1X-L'** ( $X = \text{H}$  for  $G = \text{H}$  and  $X = \text{N}$  for  $G = \text{NH}_2$ ) is evaluated as in eqn. (1) where  $E_{\text{opt}}(Y)$  is the electronic energy of system Y in its optimized geometry (binding energies are thus defined to be positive). Note that no basis set superposition error (BSSE) correction has been introduced since we focus on trends only (role of G) and BSSE is known to be small for DFT calculations with a double zeta polarisation (DZP) quality basis set.<sup>28</sup>

$$\Delta_{\text{bind}}^{\text{X}} E(L') = E_{\text{opt}}(\mathbf{1X}) + E_{\text{opt}}(L') - E_{\text{opt}}(\mathbf{1X-L'}) \quad (1)$$

## Results and discussion

### G = H: Hydrogen bond?

**Aqua complex:**  $L' = \text{H}_2\text{O}$ . Benzo[*h*]quinoline reacts smoothly with the complex  $[\text{Ir}(\text{cod})(\text{PPh}_3)_2]\text{BF}_4$  and hydrogen gas in moist  $\text{CH}_2\text{Cl}_2$  to give the cyclometallated complex **2H**,<sup>10</sup> a rare example both of an organometallic aqua species and of an aqua hydride complex.<sup>29,30</sup> The cyclometallated nature of the benzoquinoline ligand bq-H was clearly established by X-ray crystallography.<sup>11</sup> Although the hydride and the water protons were not refined, the connectivity around the metal center was characterized from NMR and IR studies:  $\text{H}_2\text{O}$  *trans* to C and H *trans* to N.

The optimized geometry for complex **2H** is shown in Fig. 1 along with some geometrical parameters. The agreement with the crystal structure is acceptable since the crystallographic determination was of only moderate quality ( $R = 8.5\%$ ). The best agreement is obtained for Ir-C (2.018 vs. 1.99(2) Å), Ir-P (2.318 vs. 2.336(7) and 2.319(7) Å), and the bite angle of the bq-H ligand (80.2 vs. 80.2(9)°). The Ir-N (2.189 vs. 2.10(2) Å) and Ir-O (2.319 vs. 2.26(2) Å) bonds are computed too long. The Ir-H bond distance (1.593 Å) is typical of iridium (iii) complexes.

The calculated binding energy  $\Delta_{\text{bind}}^{\text{H}} E(\text{H}_2\text{O})$  of the  $\text{H}_2\text{O}$  ligand is  $23.2\text{ kcal mol}^{-1}$ . This value is rather high for an aqua complex especially with a long Ir-O bond distance

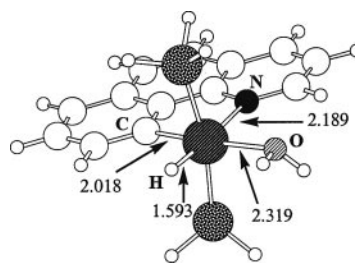


Fig. 1 Optimized geometry for the aqua complex, **2H**, with  $G = \text{H}$ . Bond distances are in Å.

(2.319 Å). This finding is in agreement with the experimental observation of tenacious binding of the aqua ligand in **2H**. Even if the reagents and solvents used are dried, the aqua complex still tends to be formed from adventitious water.<sup>11</sup>

One factor that leads to the special stability of the aqua complex can be seen from the geometry of **2H** (Fig. 1) where one O–H bond is aligned with the Ir–H bond (H–Ir–O–H dihedral angle: 4°). This “*cis* interaction” (**A** in Scheme 2) between polarized  $M^{\delta+} - H^{\delta-}$  and  $O^{\delta-} - H^{\delta+}$  bonds resembles that described by Milstein *et al.* for *cis*-[Ir(H)(OH)(PMe<sub>3</sub>)<sub>4</sub>][PF<sub>6</sub>],<sup>31</sup> where the neutron diffraction structure<sup>32</sup> shows a short O–H···H–Ir distance of 2.40(1) Å and a small Ir–O–H angle of 104.4(7)°. This orientation, reproduced by DFT calculations,<sup>33</sup> was explained by a dipole–dipole interaction.<sup>34</sup>

Although there is certainly no covalent bond between the basic hydride and the acidic proton on H<sub>2</sub>O in complex **2H** (H···H 2.642 Å), the interaction might have been viewed as a hydrogen bond, but, this “hydrogen bond”, if any, is certainly very weak both from experiment (the two Hs on H<sub>2</sub>O are equivalent by NMR even at low temperature) and from theory (the two O–H bond distances are the same: 0.966 Å). Interestingly the Ir–O–H angles are different. That for the O–H aligned with Ir–H is significantly smaller (108.6 *vs.* 117.1°). The metal–hydride bond might thus be considered as a source of weak attracting interaction. This *cis* effect<sup>35</sup> is sufficiently strong to induce a preferential orientation for an H<sub>2</sub> ligand in *cis* position with respect to M–H: in a *cis*-M(H)(H<sub>2</sub>) unit, M, H and H<sub>2</sub> are almost always coplanar.<sup>21</sup>

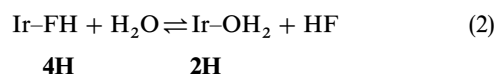
**Hydrogen fluoride complex: L' = HF.** By reaction with [nBu<sub>4</sub>N]F, the water ligand in complex **2H** is substituted by fluoride to give **3H**.<sup>14</sup> Upon protonation at –80 °C, no HF complex is obtained and the aqua complex is recovered with loss of HF. The same procedure led to the observation of an HF complex when G = NH<sub>2</sub>,<sup>13,14</sup> and is directly related to the hydrogen-bonding properties of the G group (*vide infra*).

The instability of the HF complex for G = H could then be attributed to the absence of stabilizing interaction within the complex. However, we showed for **2H** that the Ir–H bond is a source of stabilization (although weak) for the  $X^{\delta-} - H^{\delta+}$  bond. We therefore looked for possible complexation of HF to **1H** and found the ground state structure **4H** (Fig. 2). The essential feature of the optimized structure **4H** is the geometry of the HF ligand. The Ir–F bond (2.416 Å) is much longer than the usual range and in particular much longer than in the bifluoride complexes (2.124(3) Å for Mo(PMe<sub>3</sub>)<sub>4</sub>(H)<sub>2</sub>(F)(FHF)<sup>18</sup> and 2.284(5) Å for *trans*-Ru(dmpe)<sub>2</sub>(H)(FHF)<sup>19</sup>).<sup>36</sup> The Ir–F–H angle of 107.5° is smaller than the corresponding angle for Mo(PMe<sub>3</sub>)<sub>4</sub>(H)<sub>2</sub>(F)(FHF) (123.4°) indicating some attraction between the basic hydride and the acidic proton. As expected for an attractive effect, the coordinated HF in **4H** is slightly elongated in comparison with free HF (0.930 *vs.* 0.922 Å).

The binding energy  $\Delta_{\text{bind}}^{\text{H}} E(\text{HF})$  of 18.0 kcal mol<sup>–1</sup> is rather high, a result that can not entirely be attributed to the *cis* effect. We have therefore tried to estimate the magnitude of

the stabilizing *cis* attraction by Ir–H. Rotating the HF ligand by 180° around the Ir–F bond removes the *cis* interaction. A geometry, **4H-TS**, was optimized as a transition state on the potential energy surface. The motion along the coordinate associated with the imaginary frequency corresponds to a departure of the HF ligand from the bq plane to yield back **4H**. The geometry of the HF ligand in the TS confirms the absence of *cis* attraction (Ir–F 2.437, H–F 0.928 Å, and Ir–F–H 124.3°). The relative energy of +3.1 kcal mol<sup>–1</sup> for **4H-TS** with respect to **4H** gives an estimate of the stabilizing energy associated with the *cis* effect which gives only a small contribution to the total binding energy (18.0 kcal mol<sup>–1</sup>).

The coordination of HF being thermodynamically favored, why have so few systems been characterized? In the particular case of **4H** a key point is that the binding energy of H<sub>2</sub>O is stronger and the equilibrium (2) is shifted to the right. The reaction energy of –5.2 kcal mol<sup>–1</sup> is large enough for the thermal population of **4H** to be negligible (<<1%), and moreover free HF is very reactive toward glassware. The equilibrium is then probably completely shifted to the right.



To isolate an HF complex it is necessary both to increase the binding energy and to protect the acidic proton from any adventitious base. The key is to design a system with a strong hydrogen-bonding capability. The basic group must not be too strong however, or the proton will transfer to the base and we will no longer have an HF complex.

**G = NH<sub>2</sub>: Hydrogen bond!**

**Fluoride complex: L' = F<sup>–</sup>.** The aqua complex **2N** reacts with [nBu<sub>4</sub>N]F to yield the fluoride complex Ir(H)(F)(bq–NH<sub>2</sub>)(PPh<sub>3</sub>)<sub>2</sub> **3N**.<sup>13,14</sup> The crystal structure for **3N** does not show the hydrogen atoms and, in particular, does not permit structural characterization of the hydrogen bonding pattern.<sup>14</sup>

The optimized geometry for complex **3N** (Fig. 3) is in very good agreement with the crystal structure. The NH<sub>2</sub> group is almost planar and the nitrogen lone pair conjugates with the bq rings as illustrated by the short C2–N2 bond (1.348 Å). The G group and the vacant site in **1** define a “binding cavity” where two-point binding of L' with Ir and G may occur.<sup>38</sup> The NH<sub>2</sub> hydrogens are labeled H<sub>endo</sub> (toward the vacant site) and H<sub>exo</sub> (away from the vacant site). From the optimized structure for **3N** (Fig. 3) there is clearly an F···H–N hydrogen bond, in agreement with the experimental results. The N–H<sub>endo</sub> bond is noticeably elongated compared to N–H<sub>exo</sub> (1.051 *vs.* 1.005 Å). The F···H distance of 1.560 Å is consistent with the observed *J*(F,H) coupling constant of 52 Hz at 193 K. In the optimized structure **3N** the two NH<sub>2</sub> protons are inequivalent as observed by NMR at low temperature.

Having established the existence of an F···H–N hydrogen bond in complex **3N** we now turn to the estimation of the strength of this bond. Experimentally, this is usually done by VT NMR experiments in which the two NH<sub>2</sub> protons are different at low temperature but become equivalent at room temperature. The Gibbs energy of activation  $\Delta G^\ddagger$  for H exchange (12.4 kcal mol<sup>–1</sup>) gives an estimate of the strength of the hydrogen-bond after correction for the intrinsic rotation barrier around the C–N bond.<sup>8</sup>

This correction procedure is easily carried out through calculations by locating the appropriate transition states for rotation around the C–N bond. Starting from **1N** (vacant site *trans* to C) the NH<sub>2</sub> group can be rotated in two ways (Fig. 4). The structure **1N-TS<sub>endo</sub>**, optimized as a transition state (i209 cm<sup>–1</sup>), contains a nitrogen lone pair pointing toward the vacant site (*endo* position, Fig. 4). A second transition state **1N-TS<sub>exo</sub>** (i355.9 cm<sup>–1</sup>) has a nitrogen lone pair pointing away

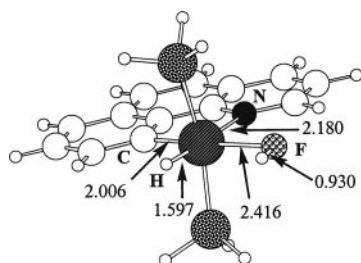
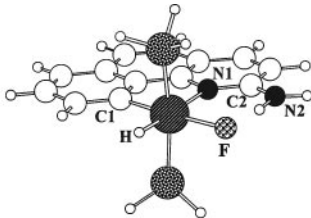


**Fig. 2** Optimized geometry for the hydrogen fluoride complex, **4H**, with G = H. Bond distances are in Å.



	Exp.	Calc.
Ir-C1	2.009	2.028
Ir-F	2.143	2.123
Ir-N	2.168	2.181
Ir-P	2.305	2.295
N1-C2	1.331	1.351
C2-N2	1.343	1.348
C1-Ir-N1	80.3	79.9
C1-Ir-F	174.8	173.6
N1-Ir-F	95.5	93.7
P-Ir-P	170.4	170.6
N1-C2-N2	117.7	117.5
N2-H <sub>endo</sub>		1.051
N2-H <sub>exo</sub>		1.005
F-H <sub>endo</sub>		1.560
F-H <sub>endo</sub> -N2		166.3

**Fig. 3** Optimized geometry for the fluoride complex, 3N, with G = NH<sub>2</sub> and comparison with geometrical parameters for the corresponding experimental structure (PPh<sub>3</sub>).<sup>14</sup> Bond distances are in Å and angles are in degrees.

from the vacant site (*exo* position, Fig. 4). As expected, the interaction between the nitrogen lone pair and the vacant site in 1N-TS<sub>endo</sub> favors this structure over the other one 1N-TS<sub>exo</sub>: +4.3 vs. +8.8 kcal mol<sup>-1</sup>. It is interesting that it costs only 4.3 kcal mol<sup>-1</sup> to reach a geometry (1N-TS<sub>endo</sub>) ideally suited for hydrogen bonding interaction with an incoming ligand L' (*vide infra*).

Two similar transition states for H exchange, 3N-TS<sub>endo</sub> (i489 cm<sup>-1</sup>) and 3N-TS<sub>exo</sub> (i501 cm<sup>-1</sup>), were located (Fig. 5). Owing to the lone pairs of the fluoride ligand, lone pair-lone pair repulsion may be present in the transition state. It is therefore not surprising to obtain an inversion of the TS order with 3N-TS<sub>endo</sub> lying at +29.9 kcal mol<sup>-1</sup> above 3N and 3N-TS<sub>exo</sub> lying at +17.3 kcal mol<sup>-1</sup>. The latter is in fair agreement with ΔG<sup>‡</sup> = 12.4 kcal mol<sup>-1</sup> for H exchange at 193 K in 3N (VT NMR). If the calculated 3N-TS<sub>exo</sub> is stabilized by hydrogen bonds to CD<sub>2</sub>Cl<sub>2</sub> solvent experiment and theory can be reconciled.

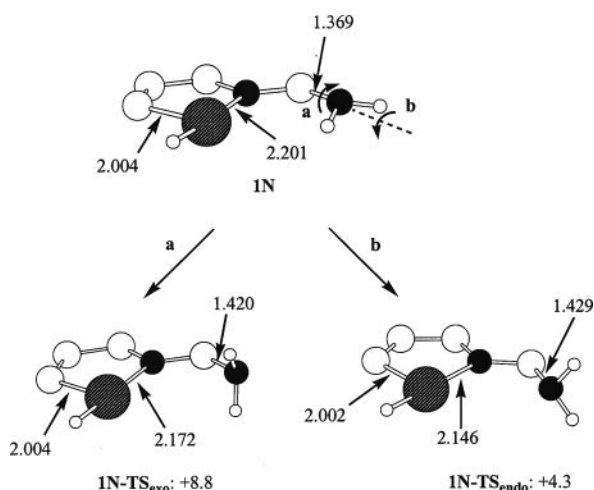


**Fig. 4** Transition states for NH<sub>2</sub> rotation in the complex with L = vacant site and G = NH<sub>2</sub>, 1N. See text for definition of *endo* and *exo*; energies in kcal mol<sup>-1</sup>.

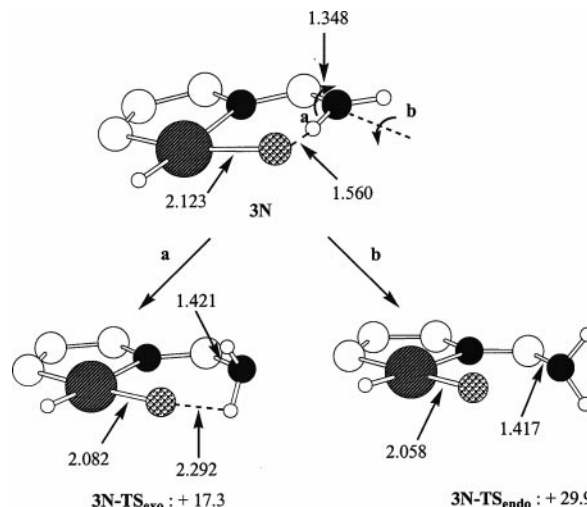
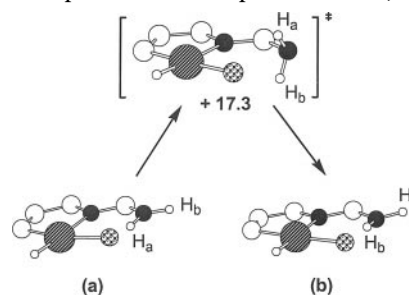


**Fig. 5** Transition states for NH<sub>2</sub> rotation in the complex with fluoride ligand and G = NH<sub>2</sub>, 3N. Details as in Fig. 4.

The exchange mechanism for the two Hs of NH<sub>2</sub> does not require a 360° rotation around the C–N bond. A 180° rotation through 3N-TS<sub>exo</sub> is sufficient to achieve exchange (Scheme 3). With equivalent phosphine ligands, configurations (a) and (b) are enantiomeric and thus equivalent in NMR studies in an achiral solvent.

The difference in relative energy for 3N-TS<sub>endo</sub> and 3N-TS<sub>exo</sub> illustrates the concept of transition-state stabilization.<sup>9</sup> The lower activation energy for 3N-TS<sub>exo</sub> arises from a conjunction of two factors: the absence of lone pair-lone pair repulsion and the presence of a hydrogen bonding interaction between F and both N–H bonds. From the relative energies of the four TS, the following semi-quantitative scheme can be derived: ΔE<sub>rot</sub> + ΔE<sub>lp,vs</sub> = 4.3; ΔE<sub>rot</sub> = 8.8; ΔE<sub>rot</sub> + ΔE<sub>lp,lp</sub> + ΔE<sub>H-bond</sub> = 29.9; ΔE<sub>rot</sub> + ΔE<sub>H-bond</sub> = 17.3. Here ΔE<sub>rot</sub> is the intrinsic rotation barrier for NH<sub>2</sub>, ΔE<sub>lp,vs</sub> the stabilizing (negative) energy associated with lone pair-vacant site interaction in 1N-TS<sub>endo</sub>, ΔE<sub>H-bond</sub> the energy of the hydrogen bond in 3N lost in both TS (3N-TS<sub>endo</sub> and 3N-TS<sub>exo</sub>), and ΔE<sub>lp,lp</sub> the lone pair-lone pair repulsion introduced in 3N-TS<sub>endo</sub>. The neglect of the weak hydrogen-bonding (2.292 Å) stabilizing term in 3N-TS<sub>exo</sub> leads to a slight overestimation of the lp-lp repulsion. We thus obtain the following values: ΔE<sub>rot</sub> = 8.8, ΔE<sub>lp,vs</sub> = -4.5, ΔE<sub>lp,lp</sub> = 12.6 and ΔE<sub>H-bond</sub> = 8.5 kcal mol<sup>-1</sup>. The strength of the hydrogen bond in complex 3N can thus be estimated as 8.5 kcal mol<sup>-1</sup> in agreement with estimated values in related systems.<sup>6,39</sup>

**Hydrogen fluoride complex: L' = HF.** In their classic 1958 text, Basolo and Pearson<sup>40</sup> indicate that the acid catalysis of fluoride substitution in cobalt (III) complexes implies that the fluoride ligand can be protonated to give a transient hydrogen fluoride complex of the type M–F–H, which rapidly loses HF. Protonation of the pendant amine fluoro-complex, 3N, with HBF<sub>4</sub>·Et<sub>2</sub>O at 195 K in CD<sub>2</sub>Cl<sub>2</sub> leads to formation of the protonated form, 4N, in solution (Scheme 1).<sup>13,14</sup> The complex decomposed on attempted isolation, but the <sup>1</sup>H



**Scheme 3**

NMR data at 183 K of **4N** indicated it is a hydrogen fluoride complex. The key observation is the presence of a  $^1J(\text{H},\text{F})$  coupling of 440 Hz consistent with **4N** being a true  $\text{N}\cdots\text{H}\cdots\text{F}$  complex, rather than having a hydrogen-bonded  $\text{N}\cdots\text{H}\cdots\text{F}$  system as in **3N** ( $^1J(\text{H},\text{F}) = 52$  Hz).

The existence of the HF complex being established, we turn to DFT calculations to predict its structure. The optimized geometry of the complex clearly exhibits a coordinated HF molecule interacting with the amino group (Fig. 6). The essential features are entirely consistent with those deduced from the spectral data but we can now also predict the key metric parameters. The H–F ligand lies in the “binding cavity” with an  $\text{F}\cdots\text{H}\cdots\text{N}$  bond to G. The H–F distance of 1.042 Å is slightly longer than that of monomeric HF (0.922 Å),<sup>41</sup> but much shorter than the  $\text{F}\cdots\text{H}_{\text{endo}}\cdots\text{N}$  distance (1.560 Å) in the neutral system **3N**. The formation of an H–F bond has also resulted in a significant elongation of the Ir–F bond (from 2.123 Å in **3N** to 2.262 Å in **4N**). However the variation is much smaller for  $\text{G} = \text{NH}_2$  than for  $\text{G} = \text{H}$  where the Ir–F bond elongates from 2.072 Å for **3H** to 2.416 Å for **4H** as a result of a stronger HF bond (0.930 Å).

The distance between N and the H of HF (1.43 Å) is considerably longer than in the two normal N–H covalent bonds (1.021 Å). This is entirely consistent with the description of **4N** as an HF complex. The  $\text{F}\cdots\text{N}$  distance of 2.470 Å is much shorter than the  $\text{F}\cdots\text{N}$  distance found experimentally (X-ray) for the fluoride complex **3N** (2.674 Å). The N–H–F angle of 175° is in excellent agreement with the linear arrangement usually preferred for hydrogen bonding given the constraints of the bonding site. The marked pyramidalization of N certainly increases the Lewis basicity of the lone pair involved in the hydrogen bond.

The calculated binding energy  $\Delta_{\text{bind}}^{\text{N}} E(\text{HF})$  of 28.2 kcal mol<sup>−1</sup> in complex **4N** is very much higher than for  $\text{G} = \text{H}$  (18.0 kcal mol<sup>−1</sup>) consistent with the presence of additional stabilization as a result of hydrogen bonding. We can qualitatively estimate the hydrogen bonding contribution. The intrinsic binding energy of HF to Ir is 15 kcal mol<sup>−1</sup> as deduced from **4H-TS** where the *cis* interaction with Ir–H is absent. The hydrogen bonding strength in **4N** is best evaluated with **1N-TS**<sub>endo</sub> as a reference (having a similar orientation of the  $\text{NH}_2$  group). The total binding energy is therefore 32.5 kcal mol<sup>−1</sup> from which the intrinsic binding energy of HF needs to be subtracted. This yields a qualitative estimate

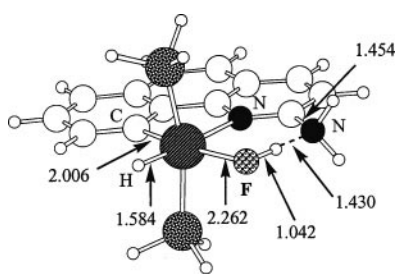


**Fig. 6** Optimized geometry for the hydrogen fluoride complex, **4N**, with  $\text{G} = \text{NH}_2$ . Bond distances are in Å.

**Table 1** Results of the AIM analysis (in atomic units) for complexes **4H** and **4N**. Only properties at selected bond critical points are shown.  $\rho_b$  is the value of the density,  $\nabla\rho_b^2$  the Laplacian of the density,  $\varepsilon$  the ellipticity, and  $H_b$  the electron energy density all calculated at the corresponding critical point

Bond	<b>4H</b>				<b>4N</b>			
	$\rho_b$	$\nabla\rho_b^2$	$\varepsilon$	$H_b$	$\rho_b$	$\nabla\rho_b^2$	$\varepsilon$	$H_b$
Ir–H	0.1549	0.0744	0.0590	−0.0867	0.1607	0.0484	0.0613	−0.0929
Ir–F	0.0355	0.1805	0.0316	−0.002 68	0.0541	0.267	0.240	−0.0048
F–H	0.3574	−2.730	0.0028	−0.7660	0.2426	−0.8965	0.0036	−0.3344
$\text{N}\cdots\text{H}$	—	—	—	—	0.1075	−0.0107	0.0049	−0.0618

of the hydrogen bond in **4N** of 17.5 kcal mol<sup>−1</sup>. The value is doubled by comparison to **3N** (8.5 kcal mol<sup>−1</sup>) in agreement with N being a better base than F and HF being a better acid than  $\text{RNH}_2$ .

To elucidate the origin of such a stabilization we have carried out an Atoms in Molecules<sup>43</sup> analysis (AIM) of the electron density for the two HF complexes **4H** and **4N**. The important result (Table 1) from this analysis is the existence of bond critical points for **4N** for both F–H and  $\text{H}\cdots\text{N}$  bonds. However the two bonds are not of the same type. The electron density  $\rho_b$  at the critical point is much higher for F–H (Table 1). The Laplacian of the density also shows that more electron density has accumulated in the vicinity of the critical point for F–H (more negative value). Finally, the electron energy density is clearly more negative for F–H than for  $\text{N}\cdots\text{H}$ . This is a sign of increased covalent character of the bond.<sup>44</sup> Therefore we can conclude that, in **4N**, there is clearly a hydrogen bond as illustrated by the presence of two critical points. The hydrogen bond can best be described as  $\text{F}\cdots\text{H}\cdots\text{N}$  with a covalent bond between F and H and a donor/acceptor type of bond between H and N.

Moreover, the AIM analysis for complex **4H** does not show any critical point between the hydride and the acidic H of HF. The *cis* interaction is thus best described as a dipole–dipole interaction between polarized bonds. The presence of the amino group in **4N** has completely reversed the geometrical preference by creating the  $\text{F}\cdots\text{H}\cdots\text{N}$  hydrogen bond. We have tried to optimize the complex  $\text{Ir}(\text{H})(\text{F})(\text{bq-NH}_3^+)(\text{PH}_3)$  with an  $\text{N}\cdots\text{H}\cdots\text{F}$  hydrogen bond but the system always returned to **4N**. This is consistent with N being a better hydrogen bond acceptor than F, and H–F being a better hydrogen bond donor than N–H. The case of  $\text{L}' = \text{H}_2\text{O}$  is somewhat analogous in this respect and also shows the dichotomy of hydrogen bond acceptor/hydrogen bond donor power, to a lesser extent however.

#### Weaker hydrogen bonds in water compound: $\text{L}' = \text{H}_2\text{O}$ .

Experimentally, the detailed structure of the aqua complex **2N** was not well determined from  $^1\text{H}$  NMR spectroscopy.<sup>14</sup> At 25 °C the protons of the  $\text{bq-NH}_2$  are equivalent, and free and bound  $\text{H}_2\text{O}$  undergo fast exchange. At −80 °C the free/bound  $\text{H}_2\text{O}$  exchange is frozen out and the bound  $\text{H}_2\text{O}$  appears in the form of two resonances in 1 : 1 ratio. The  $\text{bq-NH}_2$  appears as a single resonance at all temperatures. Therefore structure **B** (Scheme 2) was weakly preferred from the experimental observations. A theoretical study of the dynamics of H exchange was thought necessary to put our understanding of the NMR results on a firmer footing.

We now find the predicted ground state structure for complex **2N** is best described as structure **B** (Scheme 2 and Fig. 7). The essential feature of the structure is the presence of an  $\text{O}\cdots\text{H}\cdots\text{N}$  hydrogen bond. Each O–H bond is different ( $\text{O-H}_{\text{endo}}$  1.004 and  $\text{O-H}_{\text{exo}}$  0.963 Å). The O–H–N angle of 159° is not optimal for efficient hydrogen bonding but is imposed by the steric constraints introduced by  $\text{G} = \text{NH}_2$ . The Ir–O bond (2.246 Å) is typical for a water complex.<sup>11</sup> Structure **2N** (Fig. 7) does not strictly agree with the experimental results because the four protons of  $\text{NH}_2$  and  $\text{H}_2\text{O}$  are

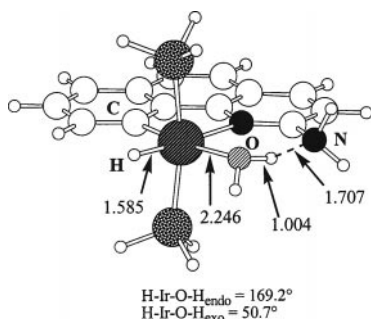


Fig. 7 Optimized geometry for the aqua complex, **2N**, with  $G = \text{NH}_2$ . Bond distances are in Å.

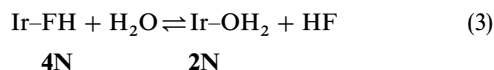
all different. As the oxygen atom is pyramidal ( $\text{H}_{\text{endo}}\text{--O--H}_{\text{exo}}$   $110^\circ$ ) the seemingly equivalent protons for  $\text{NH}_2$  are in fact diastereotopic. We next searched for possible low energy pathways for proton exchange.

The key point governing the dynamics of complex **2N** is the maintenance of stabilizing interactions in the transition states. This is in fact the case for the transition state **2N-TS<sub>N</sub>** that exchanges the Hs of  $\text{NH}_2$ . The most striking difference between **2N** and **2N-TS<sub>N</sub>** is the planarity of the  $\text{H}_2\text{O}$  ligand in the TS. The O–H bonds are still different (0.993 and 0.960 Å) showing some  $\text{O--H}\cdots\text{N}$  hydrogen bonding is maintained in the transition state. As a consequence **2N-TS<sub>N</sub>** is only 2.0 kcal  $\text{mol}^{-1}$  above **2N** indicating very easy exchange.

The transition state coordinate ( $i416\text{ cm}^{-1}$ ) corresponds to the out of plane motion of  $\text{H}_{\text{exo}}$ . The easy exchange associated with **2N-TS<sub>N</sub>** therefore keeps both protons on  $\text{H}_2\text{O}$  different while making both Hs on  $\text{NH}_2$  equivalent. The very low activation energy of 2.0 kcal  $\text{mol}^{-1}$  is consistent with the experimental observation of only one NMR peak for  $\text{NH}_2$  even down to the lowest accessible temperature ( $-80^\circ\text{C}$ ).

We could not locate a second transition state **2N-TS<sub>O</sub>** with  $\text{N--H}\cdots\text{O}$  rather than  $\text{O--H}\cdots\text{N}$  hydrogen bonding. However, a geometry with the  $\text{OH}_2$  perpendicular to the bq plane and  $\text{NH}_2$  in the plane is only 7 kcal  $\text{mol}^{-1}$  above the ground state. So the barrier for H/H' exchange in  $\text{HOH'}$  must be about the same size. In conclusion the H/H' exchange in the  $\text{NH}_2$  group is fast and one NMR peak is always seen but the H/H' exchange in the  $\text{H}_2\text{O}$  ligand is slow enough so that two peaks are seen at  $-80^\circ\text{C}$ . The exchange with free  $\text{H}_2\text{O}$  makes a quantitative estimate of the H/H' exchange barrier in the complex difficult to make but lineshape analysis shows it is close to 9 kcal  $\text{mol}^{-1}$ .

**How to isolate an HF complex?** For  $G = \text{H}$  the HF binding energy is calculated to be 18.0 kcal  $\text{mol}^{-1}$ , but for  $G = \text{NH}_2$  it is 28.2 kcal  $\text{mol}^{-1}$ . The hydrogen bonding ability of  $\text{NH}_2$  therefore stabilizes the HF complex. Surprisingly, the hydrogen bonding group has almost no influence on the binding of  $\text{H}_2\text{O}$  since the binding energy of  $\text{H}_2\text{O}$  is 24.9 kcal  $\text{mol}^{-1}$  for  $G = \text{NH}_2$  and 23.3 kcal  $\text{mol}^{-1}$  for  $G = \text{H}$ . The result is a complete change in the equilibrium between free and coordinated HF (eqn. 2 vs. 3),  $\Delta E = +3.3\text{ kcal mol}^{-1}$ .

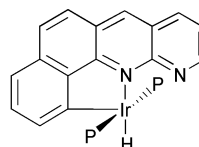


Thermodynamically, the HF complex is more stable than the  $\text{H}_2\text{O}$  complex and is the favored species at low temperature ( $G = \text{NH}_2$ ). This is in full agreement with experiment where the HF complex is observed at low temperature and dissociates upon warming. The enhanced stability of the HF complex is thus caused by the  $\text{N}\cdots\text{H--F}$  hydrogen bond.

The special topology of the binding cavity has two major consequences. The size is perfectly suited for HF hydrogen bonding ( $\text{F--H--N}$  angle of  $175^\circ$ ), but less favorable for  $\text{H}_2\text{O}$  ( $\text{O--H--N}$  angle of  $159^\circ$ ). The thermodynamic preference for the

HF complex is thus enhanced for  $G = \text{NH}_2$  both by making the HF complex more stable and making the  $\text{H}_2\text{O}$  complex less stable.

By its design, the binding cavity protects the acidic proton from external reagent and enhances the kinetic stability of the complex. The key to isolating an HF complex would be to build a binding cavity with somewhat stronger hydrogen bonding capabilities that also sterically protects the HF molecule from any incoming reagent. One possibility is a binding cavity with a nitrogen lone pair pointing towards the binding site. A bq with a fused pyridine ring (see below) should be perfect in this respect. Preliminary studies of the HF complex of this system gave a binding energy of 35.2 kcal  $\text{mol}^{-1}$ . Thus the hydrogen bond in this system is stronger than in **4N** and experimental work at Yale is underway to synthesize and try to isolate and structurally characterize this HF complex.<sup>45</sup>



## Conclusion

In this paper we predict the structure of a new type of complex that has proved too unstable for X-ray crystallography study and suggest a ligand system that might better stabilize it for future isolation. We have also shown by DFT calculations how hydrogen bonding can be a very powerful and sensitive tool to tune structure and reactivity in organometallic chemistry. With appropriate ligand design, it becomes possible to stabilize unusual species like HF selectively while *not* stabilizing the corresponding aqua complex even though it has the same structure. We find hydrogen bonding facilitates several dynamic processes. Calculations have shown how strong hydrogen bonding in one TS allows fast exchange of  $\text{NH}_2$ .

## Acknowledgements

This work was supported by the U.S. NSF, the Université de Montpellier and the CNRS. E. C. would like to thank the RSC for a generous travel grant. R.H.C. thanks the University of Montpellier for a visiting professorship. We are grateful to Dong-Heon Lee for checking the NMR spectroscopic properties of the aqua complex **2N**.

## References and notes

- R. C. Cohen and R. J. Saykally, *J. Chem. Phys.*, 1993, **98**, 6007.
- B. E. Smart, *Mol. Struct. Energy*, 1986, **3**, 141.
- D. Braga, F. Grepioni and G. R. Desiraju, *Chem. Rev.*, 1998, **98**, 1375.
- D. Braga, F. Grepioni and G. R. Desiraju, *J. Organomet. Chem.*, 1997, **548**, 33.
- L. Brammer, D. Zhao, F. T. Ladipo and J. Braddockwilking, *Acta Crystallogr., Sect. B: Struct. Sci.*, 1995, **51**, 632.
- M. J. Calhorda, *Chem. Commun.*, 2000, 801.
- E. Peris, J. C. Lee, Jr and R. H. Crabtree, *J. Chem. Soc., Chem. Commun.*, 1994, 2573.
- E. Peris, J. C. Lee, Jr., J. R. Rambo, O. Eisenstein and R. H. Crabtree, *J. Am. Chem. Soc.*, 1995, **117**, 3485.
- C. Walsh, *Enzymatic Reaction Mechanisms*, Freeman, San Francisco, 1979.
- R. H. Crabtree, M. Lavin and L. Bonnevot, *J. Am. Chem. Soc.*, 1986, **108**, 4032.
- M. Lavin, E. M. Holt and R. H. Crabtree, *Organometallics*, 1989, **8**, 99.
- D.-H. Lee, B. P. Patel, E. Clot, O. Eisenstein and R. H. Crabtree, *Chem. Commun.*, 1999, 297.
- B. P. Patel and R. H. Crabtree, *J. Am. Chem. Soc.*, 1996, **118**, 13105.

- 14 D.-H. Lee, H.-J. Kwon, B. P. Patel, L. M. Liable-Sands, A. L. Rheingold and R. H. Crabtree, *Organometallics*, 1999, **18**, 1615.
- 15 R. Kuhlman, *Coord. Chem. Rev.*, 1997, **167**, 205.
- 16 R. J. Kulawiec and R. H. Crabtree, *Coord. Chem. Rev.*, 1990, **99**, 89.
- 17 Z. Mazej, K. Borrmann, K. Lutar and B. Žemva, *Inorg. Chem.*, 1998, **37**, 5912.
- 18 V. J. Murphy, T. Hacall, J. Y. Chen and G. Parkin, *J. Am. Chem. Soc.*, 1996, **118**, 7428.
- 19 M. K. Whittlesey, R. N. Perutz, B. Greener and M. H. Moore, *Chem. Commun.*, 1997, 187.
- 20 During the completion of this work we became aware of the synthesis of a new bifluoride complex: D. C. Roe, W. J. Marshall, F. Davidson, P. D. Soper and V. V. Grushin, *Organometallics*, 2000, **19**, 4575.
- 21 F. Maseras, A. Llédos, E. Clot and O. Eisenstein, *Chem. Rev.*, 2000, **100**, 601.
- 22 M. J. Frisch, G. W. Trucks, H. B. Schlegel, G. E. Scuseria, M. A. Robb, J. R. Cheeseman, V. G. Zakrzewski, J. A. Montgomery, R. E. Stratmann, J. C. Burant, S. Dapprich, J. M. Millam, A. D. Daniels, K. N. Kudin, M. C. Strain, O. Farkas, J. Tomasi, V. Barone, M. Cossi, R. Cammi, B. Mennucci, C. Pomelli, C. Adamo, S. Clifford, J. Ochterski, G. A. Petersson, P. Y. Ayala, Q. Cui, K. Morokuma, D. K. Malick, A. D. Rabuck, K. Raghavachari, J. B. Foresman, J. Cioslowski, J. V. Ortiz, B. B. Stefanov, G. Liu, A. Liashenko, P. Piskorz, I. Komaromi, G. Gomperts, R. L. Martin, D. J. Fox, T. Keith, M. A. Al-Laham, C. Y. Peng, A. Nanayakkara, C. Gonzalez, M. Challacombe, P. M. W. Gill, B. G. Johnson, W. Chen, M. W. Wong, J. L. Andres, M. Head-Gordon, E. S. Replogle and J. A. Pople, GAUSSIAN 98, Revision A.7, Gaussian, Inc., Pittsburgh, PA, 1998.
- 23 A. D. Becke, *J. Chem. Phys.*, 1993, **98**, 5648.
- 24 J. P. Perdew and Y. Wang, *Phys. Rev. B*, 1992, **82**, 284.
- 25 D. Andrae, U. Häußermann, M. Dolg, H. Stoll and H. Preuß, *Theor. Chim. Acta*, 1990, **77**, 123.
- 26 A. Bergner, M. Dolg, W. Küchle, H. Stoll and H. Preuß, *Mol. Phys.*, 1999, **30**, 1431.
- 27 C. A. Tolman, *J. Am. Chem. Soc.*, 1970, **92**, 2953.
- 28 A. Rosa, A. W. Ehlers, E. J. Baerends, J. G. Snijders and G. te Velde, *J. Phys. Chem.*, 1996, **100**, 5690.
- 29 H. Taube, *Coord. Chem. Rev.*, 1978, **26**, 33.
- 30 R. H. Crabtree, P. C. Demou, D. Eden, J. M. Mihelcic, C. Parnell, J. M. Quirk and G. E. Morris, *J. Am. Chem. Soc.*, 1982, **104**, 6994 and references cited in this paper.
- 31 D. Milstein, J. C. Calabrese and I. D. Williams, *J. Am. Chem. Soc.*, 1986, **108**, 6387.
- 32 R. C. Stevens, R. Bau, D. Milstein, O. Blum and T. F. Koetzle, *J. Chem. Soc., Dalton Trans.*, 1990, 1429.
- 33 D. Braga, F. Grepioni, E. Tedesco, M. J. Calhorda and P. E. M. Lopes, *New J. Chem.*, 1999, **23**, 129.
- 34 J. C. Lee, Jr, A. L. Rheingold, B. Muller, P. S. Pregosin and R. H. Crabtree, *J. Chem. Soc., Chem. Commun.*, 1994, 1021.
- 35 L. S. Van der Sluys, J. Eckert, O. Eisenstein, J. H. Hall, J. C. Huffman, S. A. Jackson, T. F. Koetzle, G. J. Kubas, P. J. Vergamini and K. G. Caulton, *J. Am. Chem. Soc.*, 1990, **112**, 4831.
- 36 The long Ir–F bond length is similar to the Ag–F bond distance in  $\text{Ag} \cdots \text{FH}^+$  (2.403 Å) computed by Chattaraj and Schleyer at the MP2/6-311 + G\*\* level.<sup>37</sup>
- 37 P. K. Chattaraj and P. von Rague Schleyer, *J. Am. Chem. Soc.*, 1994, **116**, 1067.
- 38 K. Gruet, R. H. Crabtree, D.-H. Lee, L. M. Liable-Sands and A. L. Rheingold, *Organometallics*, 2000, **19**, 2228.
- 39 R. H. Crabtree, P. E. M. Siegbahn, O. Eisenstein, A. L. Rheingold and T. F. Koetzle, *Acc. Chem. Res.*, 1996, **29**, 348.
- 40 F. Basolo and R. G. Pearson, *Mechanism of Inorganic Reactions*, Wiley, New York, 1958, p. 153.
- 41 B3PWP1/6-31G\*\* optimal value for free HF for comparison with the calculated value in the complex. This value compares well with the experimental value of 0.9168 Å as deduced from IR spectra of HF in rare-gas matrices.<sup>42</sup>
- 42 M. G. Mason, W. G. von Holle and D. W. Robinson, *J. Chem. Phys.*, 1971, **54**, 3491.
- 43 R. F. W. Bader, *Atoms in Molecules*, Clarendon Press, Oxford, 1990. We have used the AIMPAC package from Bader's group available on the internet at <http://www.chemistry.mcmaster.ca/aimpac>.
- 44 D. Cremer and E. Kraka, *Angew. Chem., Int. Ed. Engl.*, 1984, **23**, 627.
- 45 R. H. Crabtree and T. Dubé, work in progress.